

Microwave Properties of Ultra-Low Loss Chromium-Doped YAG

John G. HARTNETT, Andre N. LUITEN, Jerzy KRUPKA, Michael E. TOBAR, *Senior Member, IEEE*, Pawel BILSKI

Abstract-- The microwave properties of a cylindrically cut single crystal of chromium-doped yttrium aluminum garnet ($\text{Y}_3\text{Al}_5\text{O}_{12}:\text{YAG}$) were determined between 6 K and room temperature. It exhibited very strong microwave losses near 15.3 GHz at room temperature and 15.5 GHz at 77 K. The mechanism producing the losses was found to follow standard Curie law behaviour below 30 K. In combination with the thermal expansion of the material the magnetic characteristics produced turning points in the mode frequency-temperature dependence at 60 K. Analysis showed that the Cr^{3+} doping into the dielectric lattice resulted in an anisotropic static paramagnetic susceptibility, which was resolvable at temperatures below 77 K. Two excited state energy levels were confirmed, equivalent to 0.76 K and 29 K above the ground state. The lifetime of the excited state was found to be very temperature dependent and below 100 K was dominated by Raman scattering.

Index Terms—chromium-doped YAG, frequency-temperature dependence, high-Q dielectric resonator, microwave properties, paramagnetic susceptibility.

I. INTRODUCTION

The whispering gallery (WG) mode method has proved to be a very accurate method for measurements of complex permittivity of extremely low-loss dielectrics. The method has been employed for very precise measurements of real permittivity and dielectric losses of both isotropic and uniaxial anisotropic materials [1-3]. Recently, very low-loss single-crystal materials including sapphire, YAG, and rutile have been measured this way [4-6].

In this research, a pure YAG sample (previously used in [6]) was compared to a YAG crystal of similar dimensions doped with Cr^{3+} ions. The chromium ion concentration estimated to be about 0.1% by weight, with a mixture of Cr^{3+} and Cr^{4+} ions present. The latter is not paramagnetic and is expected to induce only small changes to the dielectric properties, which will be ignored in this paper. From this research, a Cr^{3+} ion concentration of about 0.1% is consistent with the observed effects. The pure sample was transparent whereas the doped sample was a very dark green

color.

In this paper we hope to present a 'complete' measurement of the electrical and magnetic properties of Cr:YAG in the microwave domain. We present these properties in terms of the loss tangent ($\tan \delta$) where we have assumed that this parameter to be isotropic, the temperature dependence and value of the permittivity, the temperature and frequency dependence of the anisotropic components of real (dispersive) and imaginary (lossy) parts of the magnetic susceptibility. Finally, we use the measurements of the real and imaginary parts of the magnetic susceptibility to determine the relaxation time of the excited spin state and relate this to the various relaxation channels possible in this material.

Previous research [6] has shown that pure YAG loss tangent is isotropic. Through doping Cr^{3+} ions replace gallium (Ga) sites in the YAG lattice. These add additional losses, which are seen in the imaginary part of the magnetic susceptibility. However, the Cr^{3+} ion enters predominantly a site of sixfold cubic coordination with a slight trigonal distortion along the crystal [111] direction [7]. Also the thermal expansion coefficients of YAG near room temperature are not identical in the different crystal directions [8]. These facts seem to define an anisotropy axis in the crystal, which may be observable in the magnetic susceptibility. It was part of this investigation to see if the inclusion of the Cr^{3+} ions would indicate any anisotropy in the lattice.

II. MEASUREMENT PROCEDURE

A. Whispering Gallery mode method

The most effective way to eliminate conductor losses in accurate dielectric loss tangent measurements is to use high-order WG modes in cylindrical specimens of the material under test. In order to evaluate the permittivity tensor components of a uniaxial anisotropic material, a cylindrical specimen is made with its crystal axis aligned to the cylinder axis. Then two WG modes are chosen that exhibit quasi-TE (H-mode) and quasi-TM (E-mode) electromagnetic field structures. Finally, a system of two nonlinear determinant equations is solved to evaluate permittivity tensor components. From permittivity components, resonance frequencies for several other modes are computed and compared with experiment to check the validity of the mode identification. For a more thorough explanation of the method refer to references [1-3].

Manuscript received November 15, 2001. This work was supported by the Australian Research Council.

J. G. Hartnett, A. N. Luiten, M. E. Tobar and P. Bilski are with the Frequency Standards and Metrology research group, Physics Dept, the University of Western Australia (telephone: 61-8-9380-3443, e-mail: john@physics.uwa.edu.au).

J. Krupka is with Institute of Microelectronics and Optoelectronics, Department of Electronics, Warsaw University of Technology, Warsaw, Poland (e-mail: krupka@imio.pw.edu.pl).

B. Loss Tangent

Once permittivity components are found, dielectric loss tangents are evaluated as solutions to the equations

$$Q_{(E,H)}^{-1} = p_{\epsilon_{\perp}}^{(E,H)} \tan \delta_{\perp} + p_{\epsilon_{\parallel}}^{(E,H)} \tan \delta_{\parallel} + p_{m_{\perp}}^{(E,H)} \chi''_{\perp} + p_{m_{\parallel}}^{(E,H)} \chi''_{\parallel} + \frac{R_s}{G^{(E,H)}} \quad (1)$$

where $\tan \delta_{\perp}$ and $\tan \delta_{\parallel}$ are the dielectric loss tangents perpendicular and parallel to the anisotropy axis; $p_{\epsilon_{\perp}}^{(H)}$, $p_{\epsilon_{\parallel}}^{(H)}$, $p_{\epsilon_{\perp}}^{(E)}$, $p_{\epsilon_{\parallel}}^{(E)}$ are the electric energy filling factors perpendicular and parallel to the anisotropy axis of the resonant structure, and $p_{m_{\perp}}^{(H)}$, $p_{m_{\parallel}}^{(H)}$, $p_{m_{\perp}}^{(E)}$, $p_{m_{\parallel}}^{(E)}$ are the respective magnetic energy filling factors, for quasi-TM WGMs (superscript E) and quasi-TE whispering gallery modes (superscript H). $G^{(E)}$ and $G^{(H)}$ are the geometric factors for quasi-TM and quasi-TE respectively. The parameters χ''_{\perp} , χ''_{\parallel} represent the imaginary part of the magnetic susceptibility resulting from the paramagnetic ions. It is assumed here that only one paramagnetic species (Cr^{3+}) is present. In a ‘‘pure’’ sample small impurities of this type cause losses that are only significant at helium temperatures. The geometric factors can be evaluated but for high enough frequencies they may be neglected entirely as having a negligible effect on the measured Q-factor. For WG modes the shapes of resonance curves often differ from the shape of an ideal Lorentzian curve so, typically, loaded Q-factor uncertainties are about 10% [9].

In our measurements both samples were mounted at the centre of a copper cavity having two adjustable coupling loops positioned at two opposite sides of the symmetry plane of the cavity. Both loops were rotated 45° with respect to the plane of symmetry, in opposite directions to allow easy coupling to both quasi-TE and quasi-TM mode families. At room temperature, the coupling loops were adjusted symmetrically to obtain very weak coupling to higher azimuthal order modes. With decreasing temperature, the coupling coefficients remained small as the unloaded Q-factor did not increase significantly.

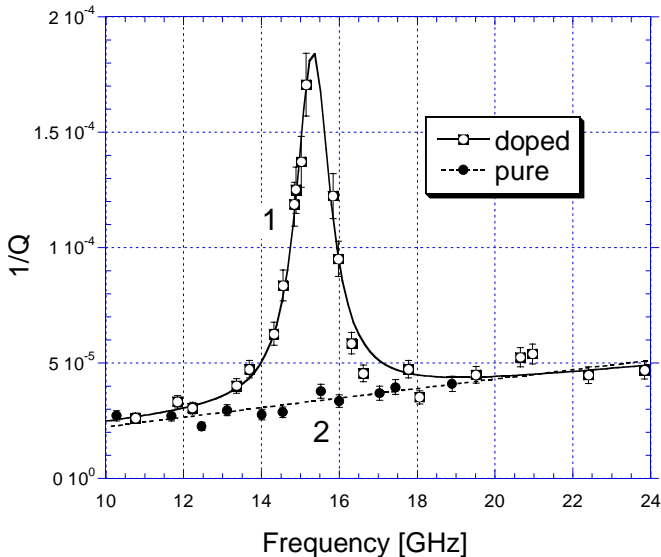


Fig. 1: Reciprocal Q-factor for WG modes measured at 300 K in the Cr^{3+} doped YAG (curve 1) and for the same modes in pure YAG (curve 2).

III. PARAMAGNETIC SUSCEPTIBILITY

A. Frequency dependence at constant temperature

Initially the resonance frequencies and Q-factors of the modes in the two fundamental families, $E_{m,1,\delta}$ and $H_{m,1,\delta}$ were determined at 300 K and at 77 K. Pure YAG was also measured and compared to these results. The reciprocal Q-factor is a measure of the loss at the mode frequency. For quasi-TE or quasi-TM modes (where electric filling factors are either 1 or 0) this represents the losses of a particular polarization either perpendicular or parallel to the crystal axis. In fig. 1, the $1/Q$ values for all measured WG modes around 15.5 GHz are presented (curve 1) with data measured in the pure YAG sample (curve 2) at 300 K. (Initially, any possible anisotropy was ignored.) The first thing to notice is the very strong electron spin resonance (ESR) line at 15.3 GHz (curve 1). Away from the spin resonance, the values of $1/Q$ in the pure and doped resonators are equal and the frequency dependence above and below the ESR line is the same. At 77 K, the spin resonance was again observed but at 15.5 GHz (curve 2 in fig. 2). Good agreement is found with published data [7, 10] at both 77 K and 300 K.

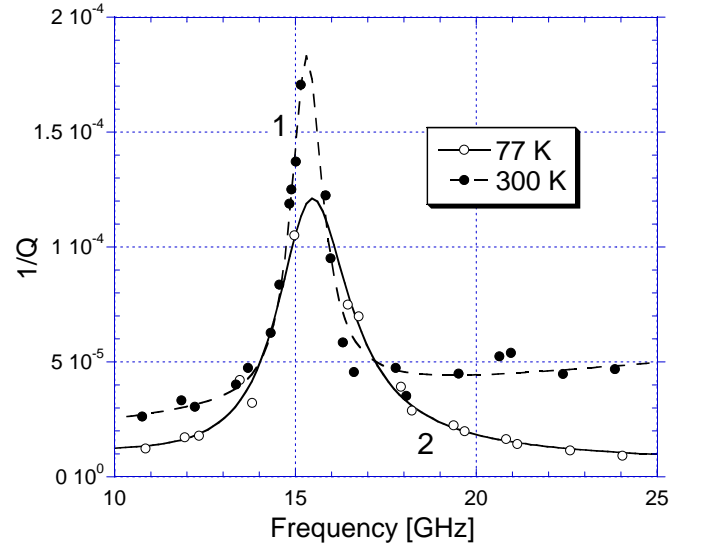


Fig. 2: Reciprocal Q-factor measurements for the same modes in the Cr^{3+} doped YAG compared at 300 K (curve 1) and at 77 K (curve 2).

Paramagnetism usually results in an ion where unpaired electrons exist in an outer orbital shell. In a crystalline solid, paramagnetic ions contribute to a net magnetic susceptibility as a result of an external magnetic field, which may be from the applied microwave signal used to interrogate the resonance in a dielectric resonator. At constant temperature, the ac susceptibility can be described as a function of frequency with a line shape [10] provided $\omega_L \approx \omega$.

$$\chi' - j\chi'' = \chi_0 \frac{T_2^2 \omega_L (\omega - \omega_L)}{1 + T_2^2 (\omega - \omega_L)^2} - j\chi_0 \frac{T_2 \omega_L}{1 + T_2^2 (\omega - \omega_L)^2} \quad (2)$$

where T_2 is the spin-spin relaxation time, ω_L is the ESR angular frequency, ω the pump angular frequency and χ_0 the static or dc susceptibility. This may be rewritten in terms of frequency (f) where the full width at half maximum (FWHM) of the Lorentzian curve, $\Delta f_L = 1/\pi T_2$. The real part is

$$\chi'(f) = \chi_0 f_L \frac{(f - f_L)}{\left(\frac{\Delta f_L}{2}\right)^2 + \left(\frac{f^2 - f_L^2}{2f}\right)^2} \quad (3a)$$

and the imaginary part

$$\chi''(f) = \chi_0 f_L \frac{\frac{\Delta f_L}{2}}{\left(\frac{\Delta f_L}{2}\right)^2 + \left(\frac{f^2 - f_L^2}{2f}\right)^2} \quad (3b)$$

B. Magnetic losses– imaginary part of susceptibility

For sufficiently high azimuthal mode numbers (m) in a WG mode, one can neglect wall losses, and (1) can be written as

$$Q_{(E)}^{-1} = p_\epsilon^{(E)} \tan \delta + p_{m\perp}^{(E)} \chi''_{\perp} + p_{m\parallel}^{(E)} \chi''_{\parallel} \quad (4a)$$

$$Q_{(H)}^{-1} = p_\epsilon^{(H)} \tan \delta + p_{m\perp}^{(H)} \chi''_{\perp} + p_{m\parallel}^{(H)} \chi''_{\parallel} \quad (4b)$$

where all parameters are frequency dependent and $p_\epsilon = p_{\epsilon\perp} + p_{\epsilon\parallel}$, which for WG modes is near unity. The values of both electric and magnetic filling factors were calculated once the relative permittivity was known. We assumed the electric susceptibility (hence $\tan\delta$) to be isotropic [6].

Equation (4) combined with (3b) was then fit to the $1/Q$ data in fig. 2. The line width (Δf_L) was determined to be 1.0 GHz at 300 K (curve 1 in fig. 2) and 2.4 GHz at 77 K (curve 2 in fig. 2). This resulted in values for the static susceptibility of 5.2×10^{-6} at 300 K and 8.9×10^{-6} at 77 K. Away from the spin resonance line, the frequency dependence of the loss tangent at 300 K was $f^{0.9}$, which was indistinguishable from the pure sample. Compare curves 1 and 2 in fig. 1 above 20 GHz. At 77 K, the frequency dependence away from the spin resonance was not resolved from the data.

C. Real part of susceptibility

The relative permittivity was determined to be isotropic with a magnitude of 10.62 at 300 K (fig. 3) from a pair of WG modes with low azimuthal number and this was used to predict the rest. There was a significant deviation from the predicted frequencies around 15.5 GHz. The effect is best illustrated by the frequency dependence of the “effective” permittivity calculated from pairs of WG modes at different frequencies at 300 K (solid points in fig 3). The “effective” permittivity assumes the mode frequencies are determined by dielectric permittivity only. Clearly around 15.5 GHz there is a strong shift in this value. The form of the data is also a close match to the expected dispersion relation (broken line in fig. 3).

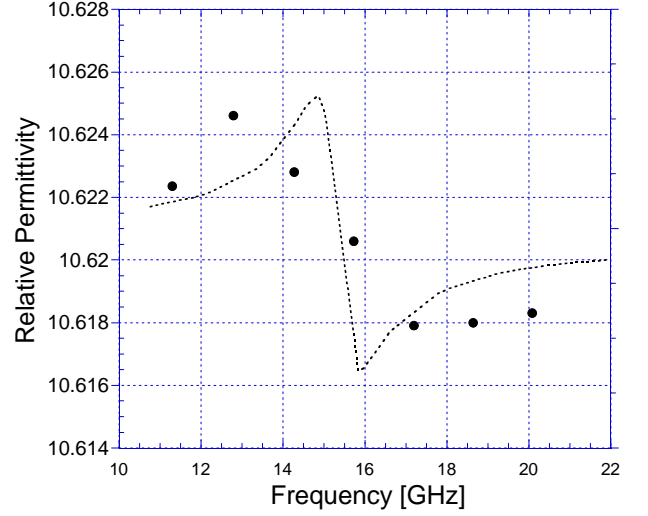


Fig. 3: The relative permittivity calculated from measured WG mode pairs as a function of frequency. A Lorentzian drawn with parameters taken from fig. 1 is also shown (as a visual guide) scaled in magnitude to fit the data.

D. Temperature dependence between 6 K and 300 K

The fractional frequency temperature dependence of a mode of resonance in a doped crystal with only one paramagnetic species can be correctly represented by

$$\frac{f_0 - f(T)}{f_0} = AT^x + C(T) \quad (5)$$

where f_0 is the expected frequency of the mode at absolute zero with no paramagnetic ions present. The value of A depends on the mode type hence the electric filling factor. The parameter x is determined from a power law fit to the pure (non-paramagnetic) crystal frequency-temperature dependence. The second term of (5) is the paramagnetic or Curie term resulting from the ac susceptibility and the magnetic-energy filling factors.

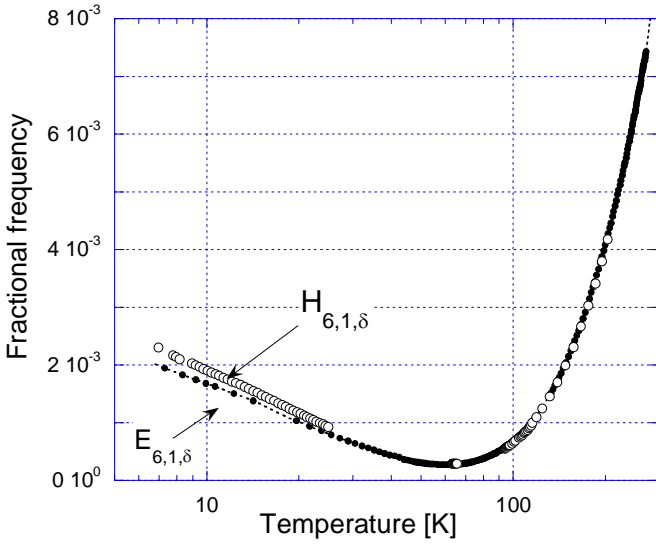
$$C(T) = \frac{1}{2} p_m \chi'(T) = \frac{1}{2} p_{m\perp} \chi'_{\perp}(T) + \frac{1}{2} p_{m\parallel} \chi'_{\parallel}(T) \quad (6)$$

which has been expanded into anisotropic components [11].

Two high-Q modes were chosen, $E_{6,1,\delta}$ (12.33 GHz) and $H_{6,1,\delta}$ (13.43 GHz). The Q value in the E mode was about twice that of the H-mode. Frequency-temperature data for these two modes was recorded continuously over a period of days as the crystal was allowed to warm slowly in a cryostat. The resonance was interrogated using a stable signal source (HP8673G synthesizer mixed with a Marconi 2031 synthesizer) and computer software that would automatically fit a Lorentzian curve to the measured power across the resonance peak [12]. The frequency data are shown in fig. 4 and the $1/Q$ data in fig. 5.

TABLE I
PARAMETERS FOR MEASURED MODES

	f_0 [GHz]	$P_{\varepsilon\perp}$	$P_{\varepsilon\parallel}$	$P_{m\perp}$	$P_{m\parallel}$
$E_{6,1,\delta}$	12.335623	0.150	0.896	0.814	0.023
$H_{6,1,\delta}$	13.469167	0.821	0.048	0.120	0.842



* All filling factors calculated at 77 K.

Fig. 4: Fractional frequency as a function of temperature for the $E_{6,1,\delta}$ mode (solid circles) and the $H_{6,1,\delta}$ mode (open circles).

Equation (5) was applied to the above data, which resulted in a value of the parameter $x = 2.84 \pm 0.14$, which is close to the value pure YAG ($x = 3.07 \pm 0.07$, taken from [6]). It was thought that the inclusion of the additional ions may alter the lattice parameters and hence the temperature dependence of the dielectric constant, although this data would exclude this at the level of a few percent. The parameter A was evaluated at 1.39×10^{-9} . The values for f_0 are listed in Table I, as are the values of both the electric and magnetic filling factors, perpendicular and parallel to the crystal axis for these two modes of interest. As a result of the anisotropic magnetic filling factors it was possible to isolate the ac paramagnetic contribution ($C(T)$) to the frequency-temperature dependence. This is shown as curve 2 in fig. 6 for the $E_{6,1,\delta}$ (12.33 GHz) mode. Curve 1 is the measured data and curve 3 is the lattice contribution described by the first term in (5).

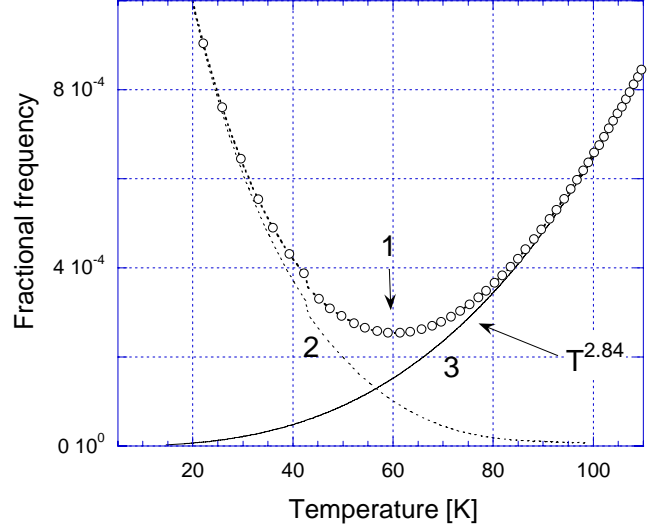
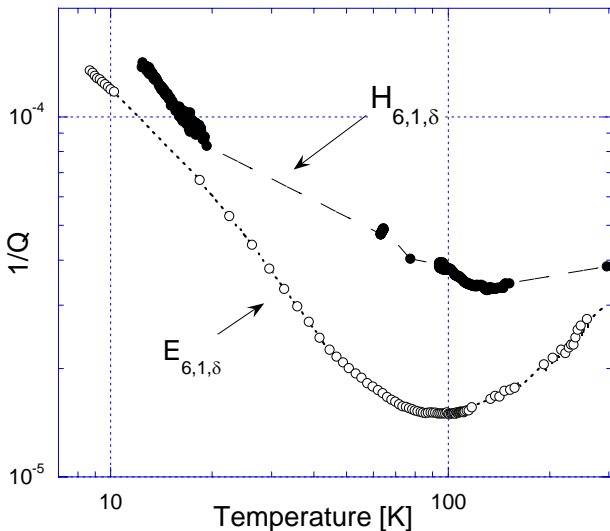


Fig. 5: Reciprocal Q-factor measured in the two WG modes as a function of temperature.

IV. LINE WIDTH

A. Relaxation rate

The parameter Δf_L , described above as the ESR line width, can be related to the lifetime of the excited state (τ) by

$$\frac{1}{\tau} = \pi \cdot \Delta f_L. \quad (7)$$

The relaxation rate is determined by a combination of the spin-spin relaxation time (T_2) and the spin-lattice relaxation time (T_1). It is clear from the line widths at 300 K and 77 K (see fig 2) that line broadening has occurred on cooling from 300 K. Spin-spin relaxation time or the dephasing time of the spin system (T_2) can be viewed as a collision process of the precessing spin. The closer the applied microwave frequency is to the ESR frequency the less frequent the collisions and this results in a cumulative excitation of the spins as they remain in phase. The spin-spin relaxation time is the average time between collisions.

Spin-lattice relaxation mechanisms cause line broadening and have been observed to fall into 3 distinct categories. At very low temperatures, a direct absorption of a microwave photon followed by the ejection of a single phonon to the lattice occurs, with $1/T_1 \sim T$. At higher temperatures, a 2-phonon resonant (Orbach) process with $1/T_1 \sim \exp(-\Delta/T)$ is observed. Here $\Delta = E_{ZFS}/k_B =$ Zero Field Splitting (energy splitting in zero applied magnetic field) divided by Boltzmann's constant. At even higher temperatures a 2-phonon non-resonant Raman scattering occurs with $1/T_1 \sim T^9$ provided the temperature is below the crystal Debye temperature. For non-Kramer's ions the latter is expected to be $1/T_1 \sim T^7$ [13]. The ground state of Cr^{3+} ion in a cubic lattice is split into a pair of Kramer's (spin degenerate) doublets [13]. In Cr:YAG a ZFS energy equivalent to $\Delta = 0.74$ K is determined by the line at 15.5 GHz from this work and [7].

Fig. 6: The measured fractional frequency (curve 1) of the $E_{6,1,\delta}$ mode below 120 K with the ac paramagnetic term (curve 2) and the lattice term (curve 3), which add to give a turning point at 60 K.

By dividing (3a) into (3b) we get an expression for the line width:

$$\Delta f_L = 2(f - f_L) \frac{\chi''}{\chi'} \quad (8)$$

The imaginary part of the susceptibility (χ'') was determined for both the E and the H-mode from the data in fig. 5. In both cases the loss tangent of the pure YAG was subtracted from the doped results for $1/Q$ using (4a) and (4b) respectively. The real part of the susceptibility (χ') was determined for both the E and the H-mode using (5) and (6) as described above. It was assumed that the ESR line frequency was constant at 15.5 GHz. The resulting data for Δf_L is shown in fig. 7, the open circles from the E-mode data and the solid circles from the H-mode data. Therefore for these analyses the static susceptibility component is determined primarily from the polarization component with the dominant magnetic field. That is, the parallel component results from the H-mode and the perpendicular component from the E-mode. This assumption is particularly good for the E-mode as the parallel component is very close to zero (see magnetic filling factors in Table I).

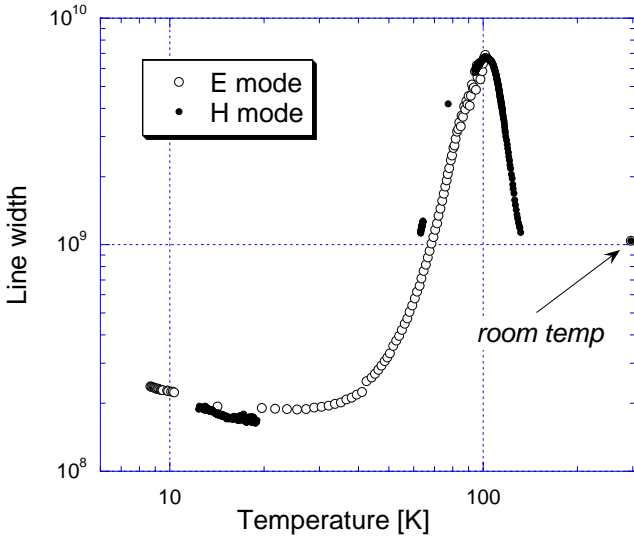


Fig. 7: The line width of the ESR line derived from the data in figs 4 and 5. The open circles are derived from the E-mode data and the solid circles from the H-mode data. Between 20 K and 80 K, fits of the form T^b result in $b = 6.7$ to 9 .

In fig. 7 a number of features are worthy of note. At low temperatures, the line width (or relaxation rate) reaches a minimum and starts to increase on decreasing temperature. At the high temperature end, a maximum is reached and the line width starts to rapidly decrease towards the room temperature point (determined from the frequency data of fig. 1). In the regime between 20 K and 80 K, the temperature dependence of the line width lies somewhere between $T^{6.7}$ and T^9 . As mentioned above, this dependence would imply a Raman two-phonon relaxation mechanism. The temperature dependence of the line width of the optical transitions at 686.4 nm and 687.3 nm are dominated by the Raman process [14]. A temperature independent line-width is observed plus a Raman scattering dependent line-width rising sharply with temperature. Fig. 3 of [14] is very similar to the 20 K and 80 K region in our fig. 7. Below 100

K, the relaxation rate may be determined predominantly by the spin-lattice time constant T_1 . Above 130 K no data was available except at room temperature, but clearly the relaxation rate approaches the room temperature value.

B. Van Vleck Paramagnetism

Calculation of the temperature dependence of the dc susceptibility (χ_0) can be simplified when the doping ions can be treated as an ensemble of non-interacting (or dilute), homogeneously distributed ions. The Cr^{3+} -doped YAG has concentration of about 0.1% Cr^{3+} -ions and may be considered dilute [13]. In this case, the temperature dependence of the paramagnetic susceptibility for a particular species is adequately described by the Van Vleck equation [15, 16]. For weak applied magnetic fields and for temperatures such that $k_B T \gg ZFS$ this reduces to the standard Curie law:

$$\chi_0 = \frac{Ng^2\mu_B^2 J(J+1)}{3k_B T} \quad (9)$$

where N is the concentration of impurity ions, g is the Landé factor which describes the multiplicity of the state, μ_B is the Bohr magneton and J is the equivalent total angular momentum of the ground state ion. For the Cr^{3+} ion in the YAG lattice the ratio of ZFS/k_B is approximately 0.74 K and as a result, (9) would apply and was found to fit the data in fig. 8 up to about 30 K. However if an additional excited state exists at higher equivalent transition temperatures the full Van Vleck equation must be used over the temperature range of the measurements. Such a state is expected at approximately 600 GHz above the ground state, which is equivalent to 28.4 K [14].

The Van Vleck equation for the three energy level system of the Cr^{3+} ion in a crystal lattice [15, 16] may be written

$$\chi_0^i = N \frac{\mu_B^2 J(J+1)}{3k_B T} \frac{\sum_n (g_i^n)^2 \exp(-\frac{\delta_n}{k_B T}) + \sum_n \alpha_n^i \exp(-\frac{\delta_n}{k_B T})}{\sum_n \exp(-\frac{\delta_n}{k_B T})}, \quad (10)$$

where $i = \perp, \parallel$ specifies the two orthogonal components of the anisotropic susceptibility, perpendicular and parallel to the crystal axis and $n = 0$ to 2 . The parameter $\delta_n = E_n - E_0$ is the ZFS energy, where E_n ($n > 0$) represents an excited state energy level and E_0 the ground state energy level. The second term in (10) is much weaker than the first and is known as the Van Vleck temperature independent paramagnetic (TIP) susceptibility and can be interpreted as a small quantum mechanical effect [17].

Making the substitution for the constant $a = \mu_B^2 J(J+1)/3k_B$ into (10) and fitting it to the data of fig. 8, resulted in the determination of the parameters listed in Table II. The fit was only valid to 70 K after which the data was not accurate due to the errors of taking the difference of small numbers as well as the deviation of Δf_L from the power law fit. The fit yielded two excited states with $\delta_1/k_B = 0.76 \pm 0.04$ K and $\delta_2/k_B = 29.3 \pm 1.0$ K. The ground state g-factors are in good agreement with published experimental values, with $g_{\parallel}^0 = 1.98$ [7] and $g_{\perp}^0 = 1.98$

[10]. The first excited state g-factors evaluated to $g_{\perp}^1 = 1.1 \pm 0.1$ and $g_{\parallel}^1 = 2.5 \pm 0.5$. The parameter g_{\parallel}^1 was insensitive to the fit and could take values up to 3, probably due to a lack of data between 25 and 60 K for the H-mode. The second excited state g-factors evaluated to $g_{\perp}^2 = 2.1 \pm 0.1$ and $g_{\parallel}^2 = (1 \pm 0.1) \times 10^{-2}$. This indicates a strong effect on the perpendicular component (hence the E-mode) and little on the parallel component. It is the main cause of the anisotropy seen in the data of fig. 8. The second excited state strongly sees the perpendicular magnetic field.

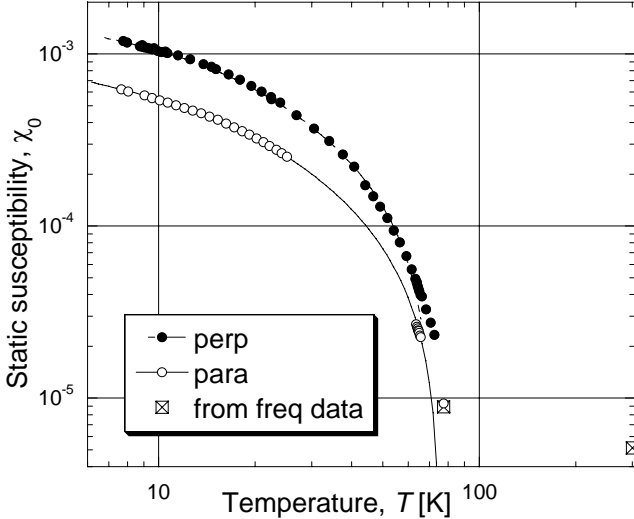


Figure 8: Anisotropic static paramagnetic susceptibility from 6 K to 300 K. The solid circles are the data for the susceptibility perpendicular to the crystal axis, and the open circles are the data for the susceptibility parallel to the crystal axis. Above 77 K it was impossible to yield any meaningful data due to curve-fitting errors. The crossed squares are the static susceptibility values derived from the curve-fits of curves 1 and 2 in fig. 2. Note that at 77 K the value derived is equal to the parallel component.

V. CONCLUSION

The introduction of Cr^{3+} ions into mono-crystalline YAG indicates an anisotropy in the magnetic properties of the material observable at temperatures below 77 K. The temperature dependent magnetic properties of the chromium ions indicate that the lattice is not completely cubic but has a small anisotropy axis. The resonant mode frequency-temperature dependence is accurately described by paramagnetic effects according to Van Vleck [15] in conjunction with the frequency changes that occur due dielectric permittivity changes. The excited state due to zero field splitting with $\delta_1/k = 0.76 \pm 0.04$ K was expected from the observed ESR line at 15.5 GHz [7]. An additional line is expected around 600 GHz [14], but was not directly excited by the available microwave signal source (≤ 26 GHz).

TABLE II
VAN VLECK CURVE FIT PARAMETERS

	g_i^0	g_i^1	g_i^2	$N \cdot \alpha_0^i$	$N \cdot \alpha_1^i$	$N \cdot \alpha_2^i$
$i = \perp$	2.0 ± 0.05	1.1 ± 0.1	2.1 ± 0.1	2.41×10^{-3}	-2.76×10^{-3}	-6.46×10^{-4}
$i = \parallel$	2.0 ± 0.05	2.5 ± 0.5	$(1.0 \pm 0.1) \times 10^{-2}$	1.86×10^{-3}	-1.37×10^{-3}	-9.92×10^{-4}
$N \cdot a$	4.85×10^{-4}					
δ_1 [K]	0.76 ± 0.04					
δ_2 [K]	29.3 ± 1.0					
N [%]	0.11					

However, it was indicated by the temperature dependence of the anisotropic static susceptibility with $\delta_2/k = 29.3 \pm 1$ K. This state is excited by thermal elevation when comparable temperatures are reached. It is also more probable in an ion when the applied magnetic field is perpendicular to the crystal axis. At low temperatures, the Q-factor of resonant modes also is limited primarily by Raman scattering of phonons in the lattice that dissipates energy to the lattice and hence the bath.

REFERENCES

- [1] J. Krupka, K. Derzakowski, A. Abramowicz, M. Tobar, and R. G. Geyer, "Complex permittivity measurements of extremely low loss dielectric materials using whispering gallery modes," presented at IEEE MTT Int. Micr. Sym. Digest, Denver, 1997.
- [2] J. Baker-Jarvis, R. G. Geyer, J. H. G. Jr, M. D. Janecic, C. A. Jones, B. Riddle, C. M. Well, and J. Krupka, "Dielectric characterization of low-loss materials," IEEE Trans. Dielectric Electric. Insul., vol. 5, pp. 571-577, 1998.
- [3] J. Krupka, K. Derzakowski, A. Abramowicz, M. E. Tobar, and R. Geyer, "Use of whispering gallery modes for complex permittivity determinations of ultra-low-loss dielectric materials," IEEE Trans. on MTT, vol. 47, pp. 752-759, 1999.
- [4] M. E. Tobar, J. Krupka, E. N. Ivanov, and R. A. Woode, "Anisotropic complex permittivity measurements of mono-crystalline rutile between 10-300 K.," Journ. of Appl. Phys., vol. 83, pp. 1604-9, 1998.
- [5] A. Luiten, M. Tobar, J. Krupka, R. Woode, E. Ivanov, and A. Mann, "Microwave properties of a rutile resonator between 2 and 10 K," Journ. Physics D: Appl. Physics, vol. 31, pp. 1383-1391, 1998.
- [6] J. Krupka, K. Derzakowski, M. E. Tobar, J. G. Hartnett, and R. G. Geyer, "Complex permittivity of some ultralow loss dielectric crystals at cryogenic temperatures," Meas. Sci. Technol., vol. 10, pp. 387-392, 1999.
- [7] J. W. Carson and R. L. White, "Zero-field splitting of the Cr^{3+} ground state in YGa and YAl garnet," Journ. Appl. Physics, vol. 32, pp. 1787, 1961.
- [8] W. Koechner, Solid-state laser engineering, vol. 1: Springer-Verlag, 1988.
- [9] J. G. Hartnett, M. E. Tobar, and E. N. Ivanov, "Optimum design of a high-Q room-temperature whispering-gallery-mode X-band sapphire resonator," unpublished., 2001.
- [10] A. E. Siegman, Microwave Solid-state Masers. New York, San Francisco, Toronto, London: MacGraw-Hill Book Company, 1964.
- [11] K. D. Bowers and J. Owen, "Paramagnetic Resonance II," in Reports on Progress in Physics, vol. 18, A. C. Strickland, Ed. London: The Physical Society, 1955, pp. 304 - 373.
- [12] A. N. Luiten, A. G. Mann, and D. G. Blair, "High resolution measurement of the temperature-dependence of the Q, coupling and resonant frequency of a microwave resonator," IOP Meas. Sci. Technol., vol. 7, pp. 949-953, 1996.
- [13] J. W. Orton, Electron Paramagnetic Resonance, 1st ed. London: Iliffe Books Ltd, 1968.
- [14] A. P. Vink and A. Meijerink, "Electron-phonon coupling of Cr^{3+} in YAG and YGG," J. Lumin., vol. 87-89, pp. 601-604, 2000.
- [15] J. H. V. Vleck, The Theory of Electric and Magnetic Susceptibilities. Oxford: Clarendon Press, 1932.
- [16] R. L. Carlin and A. J. v. Duijneveldt, Magnetic Properties of Transition Metal Compounds, vol. 2: Springer Verlag: New York, 1977.
- [17] A. R. Smith, "Anisotropic Magnetic Susceptibilities of Vanadium and Titanium ions in Corundum," : Texas Tech University, 1970, pp. 96.